


Article

A Practical Approach to Alignment and Error Feedback Control for Long-Span Arch Bridges

Xinyu Yao ^{1,*}, Chuanxi Li ¹, Longlin Wang ², Mengsheng Yu ² , Xiaoli Zhuo ², Tianzhi Hao ³ and Xirui Wang ²

¹ School of Civil Engineering, Changsha University of Science & Technology, Changsha 410114, China; lichuanxi2@163.com

² Guangxi Transportation Science and Technology Group Co., Ltd., Nanning 530007, China; gxjkqlywll@163.com (L.W.); xiaoluo19890316@163.com (M.Y.); gxjkqly@163.com (X.Z.); wangxr17@jlu.edu.cn (X.W.)

³ Guangxi Beitou Traffic Maintenance Technology Group Co., Ltd., Nanning 530029, China; htz0537@163.com

* Correspondence: xinyu1052007892@163.com; Tel.: +86-15678822242

Abstract: The accurate installation of long-span arch bridges' arch ribs remains a challenge due to the complex calculations required for cable forces and arch rib displacements, as well as the significant influence of environmental and construction loads. In this study, we propose a practical approach to alignment and error feedback control for long-span arch bridges. Cable forces were optimized using multiple control objectives based on influence matrix principles. The impact of temperature on the next segment to be installed was analyzed using the metastatic GM(1, 1) model and fitting results. Several tunable parameters were employed to account for parameter errors and environmental interference. These parameters were adjusted based on the deviations between practical and theoretical alignments for different arch rib segments, achieving a model output of an offset-free-tracking arch rib structure. This technology was applied to monitor the construction of the Tian'e Longtan Grand Bridge. Compared to conventional alignment control approaches, the proposed method achieved excellent arch ring alignment after the closure of the high-accuracy arch rib and cable release, as well as effective control of cable force uniformity and tower deviation. Field measurement data indicate that the closing deviation of the arch ring is only 3 mm. This study provides a valuable reference for the construction control of long-span arch bridges.

Keywords: long-span arch bridges; influencing matrix; the influence of temperature; feedback control



Citation: Yao, X.; Li, C.; Wang, L.; Yu, M.; Zhuo, X.; Hao, T.; Wang, X. A Practical Approach to Alignment and Error Feedback Control for Long-Span Arch Bridges. *Buildings* **2024**, *14*, 1995. <https://doi.org/10.3390/buildings14071995>

Academic Editors: Chang-Su Shim and Fabrizio Greco

Received: 9 May 2024

Revised: 15 June 2024

Accepted: 26 June 2024

Published: 1 July 2024



Copyright: © 2024 by the authors. Licensee MDPI, Basel, Switzerland. This article is an open access article distributed under the terms and conditions of the Creative Commons Attribution (CC BY) license (<https://creativecommons.org/licenses/by/4.0/>).

1. Introduction

The cable-hoisting and cable-stayed buckle method is the main method used for installing stiff frames. In this method, the stiff frame segment is lifted to a specified position through a cable; then, the segment is welded and assembled, and the internal force of the structure is adjusted through the stayed cable. This method is suitable for cases involving numerous steel frame segments [1]. Several problems are encountered as the spans of concrete-filled steel-tube arch bridges increase, as well as the number of arch rib-lifting segments. These problems include calculation difficulty, frequent adjustments of large cantilever structures, and the arching state deviation, and they emerge during the arching of the cable-stayed buckles of steel arch ribs [2–10]. Currently, the primary construction control method of arch rib installation in China is mainly based on alignment control, as it is easy to achieve alignment monitoring and stability. As such, we are faced with determining how to reasonably ascertain the cable force of arch bridges' cable-stayed buckles, as well as how to use the monitoring results during the installation of each segment to perform error feedback control. These questions have become major difficulties in monitoring the construction of long-span arch bridges.

Alignment control essentially involves the calculation and optimization of the forces of buckle cables and back cables. Currently, the cable force calculation and optimization in

the construction of arch bridges' cable-stayed buckles are mainly based on the experience of optimizing the cable force of cable-stayed bridges [11,12]. The related existing methods include the formal iterative, inversion analysis, and influencing matrix methods. For instance, Xu et al. [13] proposed an improved iterative algorithm with high computational efficiency to address the low computational efficiency typically encountered when using the formal iterative method to determine the cable tensile force of cable-stayed buckles. The improved iterative algorithm has a fast convergence speed and neglects the cable force uniformity and installation accuracy of the arch ring alignment. Owing to the unknown state parameters of a structure and the nonlinear effect of the structure during inverted demolitions, when the construction steps are complicated, it is difficult to obtain an accurate solution using this method. Qin et al. [14] and Han et al. [15] calculated the dead weight of an arch ring using the influencing matrix method. Here, for the displacement-influencing matrix under the action of the cable force of each unit, the optimization objective function was the deviation of alignment between control points and targets during construction. The deviation of the arch ring alignment and the target alignment after closing the cable was set as a constraint function. The initial tensile force of each cable in the arch ring cable-stayed buckles during construction was calculated, and the cable force uniformity was adequately controlled. However, the system was affected by the elastic deformations of the steel arch rib structure, elastic deformations of the tower, the cable's elastic modulus and thermal expansion, and many other factors [16–18]. Consequently, deviation occurs between the alignment after an actual installation and the theoretical value of the current installation, thus affecting the installation accuracy. Therefore, error correction and feedback control should be performed considering the effect of temperature and other factors to achieve an expected alignment. When calculating the cable force of the cable, the above documents ignore the variation errors of arch rib alignment and cable force caused by the deviation between the ambient temperature and the design temperature during the tension of the cable and cannot accurately determine the initial cable force. It is of great significance to study the construction control of arch rib segmental lifting, considering the influence of temperature variation and other errors for realizing the reasonable structure of the bridge.

In this paper, based on the influencing matrix principle and constrained minimization theory, combined with error feedback control theory, we propose a practical approach to alignment and error feedback control for long-span arch bridges. The proposed approach was proven theoretically and tested in practice. Specific tunable parameters were used to characterize various parameter errors and environmental interferences, and the tunable parameters were adjusted according to the deviation between the alignment and the theoretical value of each arch rib segment after actual installation. As such, an offset-free-tracking practical arch rib structure was achieved as a model output. In addition, the method was used to perform error correction and feedback control during the installation process of an arch rib, and high positioning accuracy was recorded for each arch rib segment. All kinds of parameter errors and environmental interferences during the installation of the arch rib were significantly reduced. Therefore, this study provides a reference for the construction control of long-span arch bridges. At the same time, compared with the conventional linear control method, the proposed method converges and iterates faster. At the same time, the influence of temperature and various error factors is comprehensively considered, which not only ensures that arch rib closes with high precision and the arch ring alignment after the cable loosening is maintained well but also better controls the uniformity of cable force and the deflection of towers during the construction process.

2. Mathematical Model

2.1. General Solution of Alignment Control

To meet the installation target requirements of arch rib alignments in the cable-stayed buckles of arch bridges, the one-stretch cable method or fewer cable adjustments are the methods currently used. Alignment control is essentially the calculation of the force on the cables of a cable-stayed bridge, whereas the calculation of the cable force of arch bridges

constructed by cable-stayed buckles is similar to that of cable-stayed bridges, except that the former lacks cable forces for formed bridges. However, the calculation of the cable force of arch bridges should also consider the alignment after the closure of the arch rib and paving of the bridge deck; thus, references can also be made to the cable force calculation in the construction of cable-stayed bridges [19]. The influencing matrix method is often used for cable force optimization and the determination of the cable force at the construction stage. Additionally, the effect of all structural dead loads and tensile forces is also considered in the control objectives $\{\Delta R\}$. The general equation for the initial tensile force of the cable-stayed buckles of arch bridges with a concrete-filled steel tube is given as follows:

$$[A]\{F_0\} + \{\Delta S\} = \{\Delta R\} \quad (1)$$

where $[A]$ is the unit influence matrix of the cable force adjustment on each control target, $\{F_0\}$ is the initial tensile cable force to be determined, $\{\Delta S\}$ is the displacement induced by the dead load during the installation of the arch ring cable-stayed buckles, and $\{\Delta R\}$ is the target displacement of the alignment of the designed arch bridge.

2.2. Alignment Control Optimization

This model takes the sum of the squares of the actual displacement and target displacement differences in each arch segment after loosening the cable to form an arch as the optimization objective function and the actual displacement and target displacement differences in each arch rib during the suspension assembly construction process as the constraint condition. This method is a one-time tensioning method, which avoids the disadvantages of complex calculation processes and repeated cable adjustments when using methods such as front installation and reverse dismantling to optimize the construction of arch bridge cable-stayed buckles.

The deviation between the control point u_s and target alignment u_t of displacement at the tensile stage during construction is taken as the optimization objective function. The deviation between the alignment u_n and target alignment u_t of the arch ring is taken as the constraint function after the closure of the dragon loose rope. The initial tensile force of a group of arch ring cable-stayed buckles during construction is determined and optimized, i.e., the constrained minimization problem is solved using a mathematical model. Upon assuming that the difference between the initial cable force and the optimized value is $\{\Delta X\}$, *fmincon* is used to determine the constrained nonlinear multivariable function. The *fmincon* function minimizes the *fun* function with the lower bound *lb* and upper bound *ub* of a given variable:

$$\{\Delta X\} = \text{fmincon}(\text{fun}, \{F_0\}, \begin{bmatrix} B \\ -B \end{bmatrix}, \begin{bmatrix} \Delta u + u_t - u_0 \\ \Delta u - u_t + u_0 \end{bmatrix}, lb, ub) \quad (2)$$

$$\text{fun} = \|[C]\{\Delta X\} + \{u_s - u_t\}\|^2 \quad (3)$$

where $[B]$ refers to the displacement-influencing matrix of each control point when the cable is removed under the action of the cable force, $[C]$ refers to the displacement-influencing matrix of each control point when the arch rib is installed under each unit cable force, *fun* is the objective function, $\{F_0\}$ is the initial tensile force to be solved, Δu is the limit vector of the displacement deviation of the closed loose cable under the action of the self-weight of a bare arch, u_t is the target displacement vector (displacement vector of each control point under the bare arch), and u_0 is the displacement of a control point under the initial tensile force. Then, the obtained initial tensile force is used for the formal analysis, thus resulting in the tensile force at each stage. *lb* is the lower bound of the variable $\{\Delta X\}$, and *ub* is the upper bound of the variable $\{\Delta X\}$. The initial cable force $\{F\}$ of tension after the final optimization can be determined:

$$\{F\} = \{F_0\} + \{\Delta X\} \quad (4)$$

For the nonlinearity of a long-span arch bridge, the sag effect of the cable is mainly considered at the stage of cable-stayed suspension, and the sag effect is simulated by the equivalent elastic modulus method.

Notably, in general, the newly installed component is positioned in a direction tangential to the previously installed component. For arch bridges with cable-stayed buckles, the effect of the tangential assembly displacement must be included to ensure that the finite-element calculation results are in line with the actual engineering requirements. Therefore, for arch bridges with cable-stayed buckles prone to the influence of a tangential assembly displacement, the cable force obtained by the influencing matrix method has a discrepancy with the actual tensile cable force, which requires further optimization and adjustment.

2.3. Alignment Control Considering Temperature Influence

The temperature change has a great influence on the force and deformation of bridge structures, and the results are different when the structure state is measured at different times. In order to obtain the real state data of the structure, the influence of temperature must be considered. In this paper, the morning when the temperature changes less in a day is generally taken as the collection time for the required measured data. But, there is a difference in temperature when the ribs are positioned. The temperature field generated by the arch rib and buckle system is a nonlinear temperature field under the combined effect of ambient temperature and solar radiation, and the structural error caused by temperature is cumulative. When the cantilever is extended, it deviates significantly from the design target, causing closing difficulties and affecting the internal stress and alignment of the system when the bridge is completed. During hoisting, the structural system is constantly transformed, and the stiffness also constantly changes. The hoisting segments become inconsistent under the influence of temperature. However, owing to the tangential assembling of the arch rib, a strong connection occurs between the alignment of the arch rib segments. Therefore, we can predict the influence of temperature on the arch rib of the next segment by using the measured temperature effect alignment rule of the current segment, as well as a model, to determine the efficiency.

The function $y = f(x)$ is defined at the interval $[a, b]$. At a known point a , the temperature influence rule of the $(N + 1)$ th control point is predicted by using the change in temperature of the N th control point. The grey prediction model GM(1, 1) has conditional exponential fitting. By using the original discrete data columns, a new regular discrete data column with reduced randomness is generated by one accumulation step. Then, the differential equation model is established to obtain an approximate estimate of the original data generated by the solution at the discrete points after the reduction, thus predicting the subsequent development of the original data [20–22]. The initial original data column is $x^{(0)} = (x^{(0)}(1), x^{(0)}(2), \dots, x^{(0)}(n))$; when it is accumulated once, a newly generated data column $x^{(1)} = (x^{(1)}(1), x^{(1)}(2), \dots, x^{(1)}(n))$ is obtained, where

$$x^{(1)}(m) = \sum_{i=1}^m x^{(0)}(i), m = 1, 2 \dots n. \quad (5)$$

$z^{(1)}$ is the immediate mean-generating sequence of series $x^{(1)}$, i.e.,

$$z^{(1)} = (z^{(1)}(2), z^{(1)}(3), \dots, z^{(1)}(n)) \quad (6)$$

where $z^{(1)}(m) = \delta x^{(1)}(m) + (1 - \delta)x^{(1)}(m - 1)$, $m = 2, 3 \dots n$, and $\delta = 0.5$.

$x^0(k) + az^1(k) = b$ is the basic form of the GM(1, 1) model, where b refers to the grey action quantity, a refers to the development coefficient, and the first "1" of GM(1, 1)

indicates that the equation is of the first order, while the last “1” indicates that there is only one variable.

$$\text{Let } u = (a, b)^T, Y = \begin{bmatrix} x^{(0)}(2) \\ x^{(0)}(3) \\ \vdots \\ x^{(0)}(n) \end{bmatrix}, B = \begin{bmatrix} -z^{(1)}(2)1 \\ -z^{(1)}(3)1 \\ \vdots \\ -z^{(1)}(n)1 \end{bmatrix}. \quad (7)$$

Hence, the GM(1, 1) model $x^{(0)}(k) + az^1(k) = b$ can be expressed as follows:

$$Y = Bu. \quad (8)$$

The estimated values of parameters a and b are obtained using the least squares method:

$$\hat{u} = (\hat{a}, \hat{b})^T = (B^T B)^{-1} B^T Y. \quad (9)$$

The initial value condition is $\hat{x}^{(1)}(t)|_{t=1} = x^{(0)}(1)$, based on which the following solution can be achieved:

$$\hat{x}^{(1)}(t) = \left[x^{(0)}(1) - \frac{b}{a} \right] e^{-a(t-1)} + \frac{b}{a}. \quad (10)$$

The GM(1, 1) model $x^{(0)}(k) + az^1(k) = b$ has the following solution:

$$\hat{x}^{(1)}(m+1) = \left[x^{(0)}(1) - \frac{b}{a} \right] e^{-am} + \frac{b}{a}, m = 1, 2, \dots, n-1. \quad (11)$$

To predict the original data, only the condition $m \geq n$ is sufficient. However, to improve the accuracy of the grey prediction model GM(1, 1), we set $x^{(0)}(n+1)$ as the newest information; we remove the previous information $x^{(0)}(1)$ while importing $X^{(0)}$ and let $X^{(0)} = (x^{(0)}(2), \dots, x^{(0)}(n), x^{(0)}(n+1))$. The established GM(1, 1) model is metastatic. From a prediction perspective, the metastatic model updates the information constantly; thus, it is regarded as the most ideal model. To eliminate or reduce the influence of temperature, the temperature monitored 24 h before the segment hoisting is used to correct the temperature of the next segment's arch rib hoisting, and the fitting is performed based on the original data. The influence of temperature on the arch rib of a lower segment is predicted by considering the grey prediction and fitting results comprehensively, and their adequacy and reliability are judged by the difference between the predicted data and the original data.

2.4. Feedback Control of Parameter Errors

In addition to temperature, the elastic deformations of the arch rib steel structure and tower, the elastic modulus of the cable, and other factors also affect the alignment after installation. These effects cause a discrepancy between the theoretical and actual values of the current installation stage. As the steel arch assembly proceeds, the deviation can only be adjusted by the cable force in the later stages because the cables are not adjusted once and the internal stress of the cable installed at the first stage changes constantly. Hence, a deviation occurs between the measured value of the structure and the calculated value of real-time theoretical analysis. The feedback control aims to promptly correct various parameter errors and environmental interferences during the construction of arch bridges. Using the arch rib installation test results at the current arch rib construction stage, the theoretical model is corrected to generate a fast and accurate tracking practical arch rib structure. Hence, there is deviation between the measured value of the structure and the calculated value of the real-time theoretical analysis.

Δ_x and Δ_s are the upper and lower limits of the current segment alignment caused by various error factors. By approximating the practical value after the installation of the current segment, we optimize the mathematical model (2) as follows:

$$\{\Delta X\} = fmincon(fun, \{F_0\}, \begin{bmatrix} B \\ -B \\ C \\ -C \end{bmatrix}, \begin{bmatrix} \Delta u + u_t - u_0 \\ \Delta u - u_t + u_0 \\ \Delta_s - dis_1 \\ -dis_1 + \Delta_x \end{bmatrix}, lb, ub) \quad (12)$$

According to the above analysis, the practical approach to the alignment and error feedback control is explained as follows:

- (1) The initial cable force is obtained after the final optimization. Based on the material characteristics, geometric characteristics, boundary conditions, and external load information of concrete-filled steel tube arch bridges, a finite element model is established. According to Equations (2) and (3), the initial tensile force $\{F_0\}$ of a group of buckles during construction is solved and optimized.
- (2) According to Equation (4), the cable force $\{F\}$ of a single unadjusted cable under control objectives, such as tower deviation, arch rib alignment, and cable force uniformity, is obtained.
- (3) In order to improve the accuracy of the grey prediction model GM(1, 1), the grey model GM(1, 1) with a fixed median is established, where $x^{(0)}(n+1)$ is taken as the latest information, and the previous information $x^{(0)}(1)$ is replaced with $X^{(0)}$. The model built with $X^{(0)} = (x^{(0)}(2), \dots, x^{(0)}(n), x^{(0)}(n+1))$ is called the metastatic GM(1, 1) model.
- (4) The original data are fitted, and the segment arch rib under the prediction is affected by temperature through a comprehensive consideration of metastatic GM(1, 1) and the fitting results. Then, the prediction data and the trend of the original data are used to judge whether it is reasonable and reliable.
- (5) Δ_x and Δ_s are the upper and lower limits of the current segment alignment caused by various error factors. Approximating the practical value of the current segment after installation using Δ_x and Δ_s , and optimizing the mathematical model (2), results in the feedback control characterizing various parameter errors and environmental interferences.
- (6) Through error feedback control, various parameter errors and environmental interferences in the bridge construction process are corrected. If the deviation between the measured value and the theoretical value is within a feasible region, the iteration is completed. If the requirements are not met, one should return to step (5) and adjust the tunable parameters to realize the model output, offset-free-tracking practical arch rib structure.

The steps of the practical method of linear and error feedback control are shown in Figure 1 below.

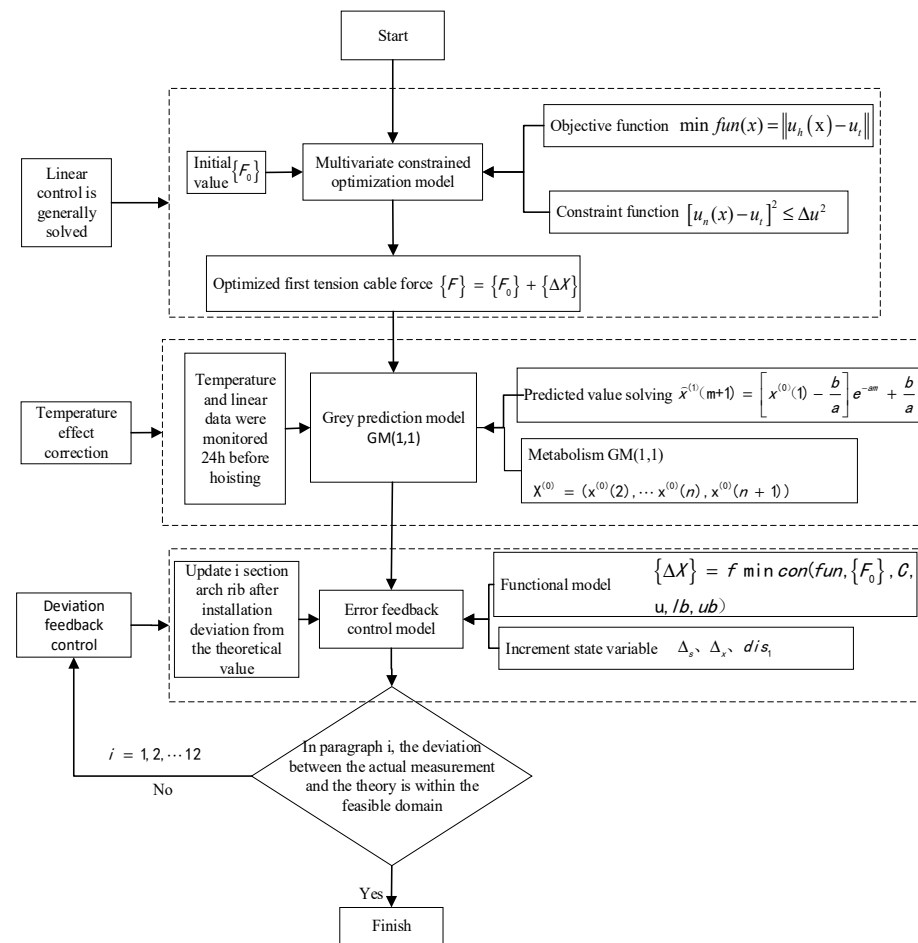


Figure 1. Flowchart of the practical approach to alignment and error feedback control.

3. Practical Application

3.1. Project Background and Finite Element Model

The Tian'e Longtan Grand Bridge is a control project of the Nandan–Tian'ao Xia-Lao Expressway. The bridge is located in Tian'ao County, Hechi City. The total length of the bridge is 2488.55 m, of which the main bridge is 624 m. The bridge scheme is of stiff-frame concrete arch bridges. The calculation span is 600 m, the cable adopts a split cable design, and the cable force at the pull end is the same as that at the anchor end. As shown in Table 1, at the construction stage, the cable forces of a single cable and two bundles of cables are set for each arch rib. The cable is made of 1860 MPa $\Phi = 15.24$ mm high-strength and low-relaxation steel strands, and the area of a single steel strand is 140 mm^2 , with an elastic modulus of $E = 1.95 \times 10^5$ MPa. A low-retraction anchor device is adopted at the anchorage end; the device is placed in the buckle structure of the end attachment of the arch rib segment. The control points are the intersection points of the upper chord axis of each arch rib and the axis of the top vertical belly bar, which are horizontally transferred to the outside part of the main chord tube during construction. The main arch ring of Tiane Longtan Bridge is installed by cable hoisting and cable-stayed buckle hanging, and the outer concrete is poured by layers of “three rings, six sections and eight working faces”. The elevation of Tiane Longtan Bridge is shown in Figure 2 below.

Table 1. Initial control commands.

Section	Manufacturing Elevation (m)	Tensile Elevation (m)	Initial Cable Force (kN)	Optimized Cable Force (kN)
1#	396.456	396.449	360	433
2#	412.811	412.789	581	593
3#	427.709	427.668	591	625
4#	444.675	444.619	749	681
5#	459.290	459.179	792	831
6#	472.252	472.112	847	878
7#	483.501	483.277	1132	1158
8#	492.950	492.718	1410	1387
9#	500.399	500.079	1722	1934
10#	505.979	505.627	2134	1981
11#	509.461	509.060	2848	2588
12#	510.881	510.394	3418	3109

**Figure 2.** Elevation of Tian'e Longtan Grand Bridge.

The total number of the nodes and elements of the finite element model of the cable-stayed buckles of the Tian'e Longtan Grand Bridge is 7614 and 15,545. The material properties, geometry, boundary conditions, and external loads are consistent with the design. Owing to the symmetrical structure of the bridge, the cables are numbered according to construction stages and sequences. The finite element model is shown in Figure 3.

**Figure 3.** Finite element model of main bridge of Tian'e Longtan Grand Bridge.

3.2. Application of the Practical Approach to Alignment Control and Error Feedback

3.2.1. General Solution and Optimization of Alignment Control

In the design review phase, after establishing the finite element model of the cable-stayed buckles in the Tian'e Longtan Grand Bridge, we extract the unit influence matrices [A], [B], and [C] of the unit cable force adjustment on each control target, the deviation between the displacement control point and the target alignment at the current tensile stage during construction, and the difference between arch ring alignment u_n after closure and target alignment u_t . Under the constraint conditions of different column deviations and

arch rib alignment errors, the optimization results are different, and the corresponding maximum cable force at the construction stage also differs. In addition, the cable force of the bridge is optimized using the proposed alignment control optimization method. Table 1 shows the tensile cable force and control commands when the cable force uniformity and safety are all considered for an arch rib alignment within 0–45 mm and a tower deviation within 0–60 mm. The segmental division of arch ribs is shown in Figure 4 below.

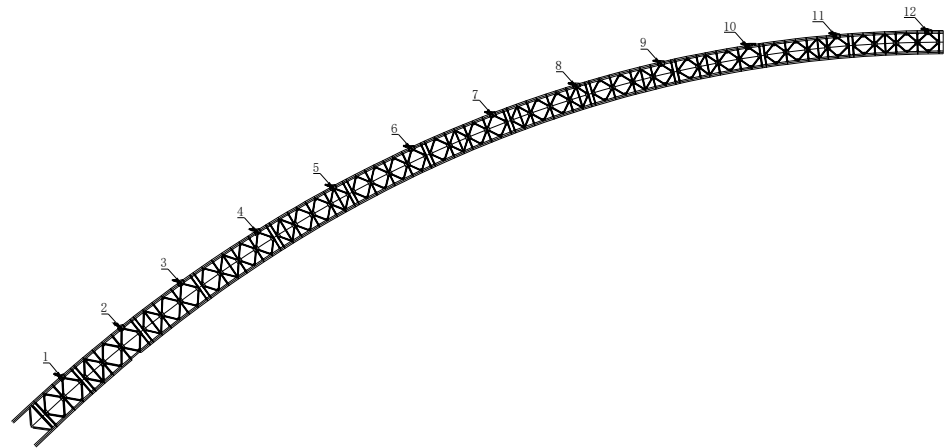


Figure 4. Arch rib segment division (The number indicates the arch rib segment number).

In the design review phase, the installation control commands in Table 1 are used and are shown in Figure 5, and the error range of each control objective is shown in Figure 6.

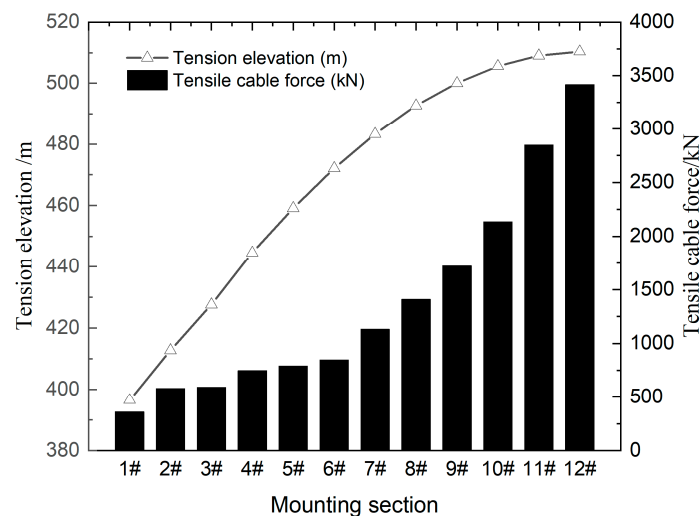


Figure 5. Installation control commands.

As shown in Figure 5, performing alignment control optimization using the proposed method solves the problems of large fluctuations in each cable force and poor cable force uniformity with the increasing number of hoisting segments. Meanwhile, the adjacent cable force changes only slightly, and the tower deviation and arch rib alignment are good, indicating that the proposed method effectively overcomes the defects of traditional construction monitoring and calculation methods, and it also effectively adjusts the parameters during the construction lifting process.

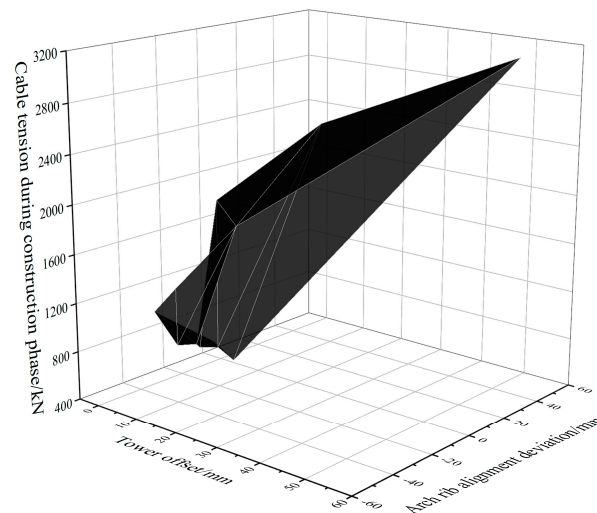


Figure 6. Error range of each control objective.

3.2.2. Alignment Control Considering Temperature

To further study the variation rules of the arch ring alignment and cable force affected by temperature during hoisting construction, the above method is used to predict the temperature effect of the arch rib alignment of the next segment using the measured data of the current segment alignment, and a new control value is given. In the hoisting of segment 6#, for example, after installing segment 5#, the alignment tested at 22:01 in the evening is taken as the initial value. In light of metastatic GM(1, 1) and the fitting data, at temperatures of 15.7 degrees Celsius and 17.9 degrees Celsius, the following is obtained:

$$X^{(0)} = (x^{(0)}(2), \dots, x^{(0)}(n), x^{(0)}(n + 1)) = (0, -2, -4, -6, -12, -19)$$

$$X^{(0)} = (x^{(0)}(2), \dots, x^{(0)}(n), x^{(0)}(n + 1)) = (-2, -1, -2, -7, -18, -34)$$

Accordingly,

$$\hat{x}^{(1)}(m + 1) = \left[x^{(0)}(1) - \frac{b}{a} \right] e^{-am} + \frac{b}{a}, m = 1, 2, \dots, n - 1$$

We obtain predicted values of -20 mm and -31 mm, respectively.

We predict the temperature effect behavior after the installation of segment 6#. The installation instructions for segment 6# are thus provided, and the measured values are compared with the predicted values after the installation of segment 6# (see Table 2):

Table 2. Prediction using the improved GM(1, 1) model and fitting results.

No.	Time	Temperature	1A/mm	2A/mm	3A/mm	4A/mm	5A/mm	Prediction 6A/mm	Post-Installation Measurement 6A/mm	Error Percentage/%
1	3-28 9:21 AM	15.7	0	-2	-4	-6	-12	-19	-20	5
3	3-28 10:31 AM	17.9	-2	-1	-2	-7	-18	-34	-31	3

After installing segment 5#, predictions are made using the improved GM(1, 1) model; the fitting results are illustrated in Figures 7 and 8.

As shown in Figures 6 and 7, after predicting the temperature influence behavior using the proposed method, the prediction errors of the metastatic GM(1, 1) model and fitting results for segment 6# are less than 5%. Temperature correction is also performed in other segments using this method, resulting in new instructions, as shown in Figure 9.

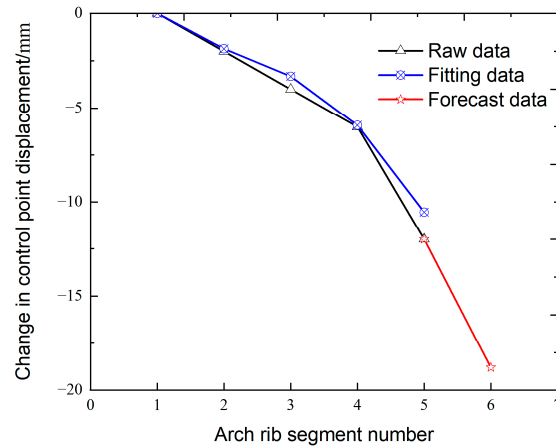


Figure 7. Prediction using metastatic GM(1, 1) model and fitting results under 15.7 °C.

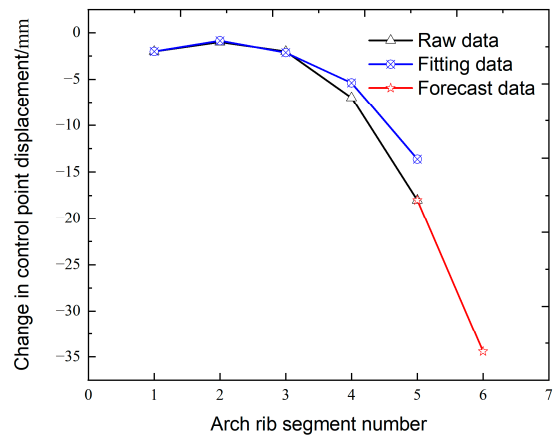


Figure 8. Prediction using metastatic GM(1, 1) model and fitting results under 17.9 °C.

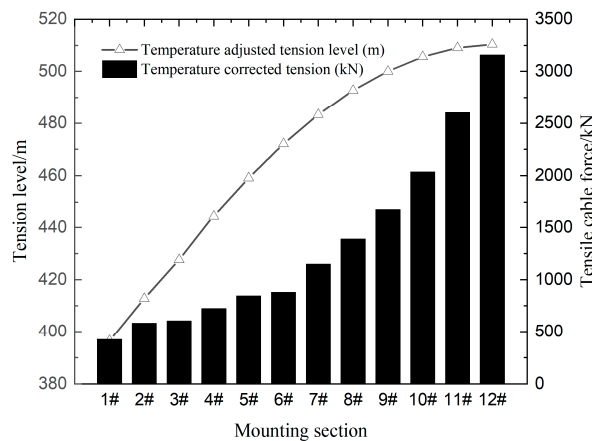


Figure 9. Installation control commands considering temperature.

3.2.3. Error Feedback Control and Control Effect Evaluation

Conventional alignment control methods are usually affected by the elastic deformation of the arch rib steel structure and tower, changes in the elastic modulus of the cable, and many other factors. Therefore, the actual alignment after installation and the theoretical value of the current installation stage differ from each other. For the large-span arch bridge, the accumulated errors of each segment during the arch formation of the cable-stayed buckle are likely to cause errors in the arch formation state. The various parameter errors

and environmental interferences were corrected using the proposed method; the resulting installation instructions for each stage are shown in Figure 10.

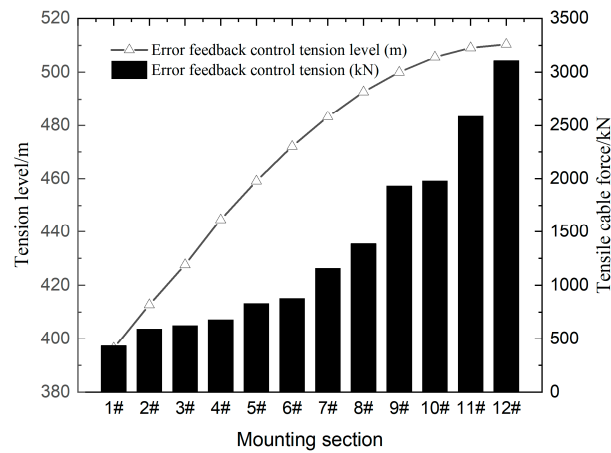


Figure 10. Control commands under feedback control of different parameter errors.

The installation of each section of arch ribs was analyzed. The closure alignment of the arch rib obtained using the practical approach to alignment and error feedback control for long-span arch bridges is shown in Figure 11. The alignment of the slack cable and alignment of the bare arch are shown in Figure 12.

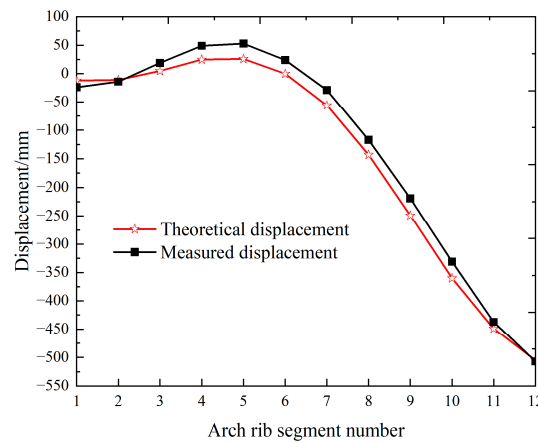


Figure 11. Closure alignment.

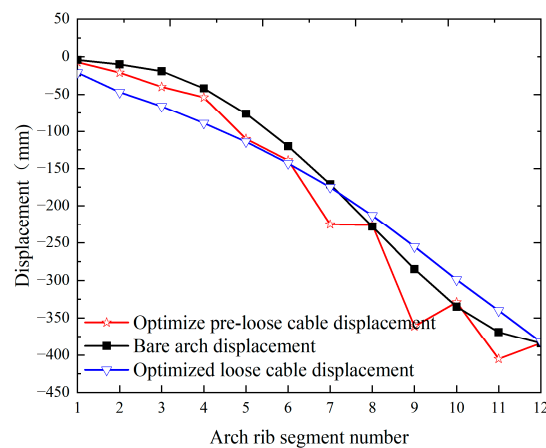


Figure 12. Slack alignment and target alignment of control points in each segment.

As shown in Figures 10 and 11, the closure alignment and the alignment of the arch rib after the cable is loosened are good, and the error between the alignment of the slack cable and the alignment of the bare arch after optimization is within 45 mm when the proposed method is used, and the result is smoother.

4. Conclusions and Recommendations

The alignment control problem considered in this study can be summarized as cable force optimization, which is different from the existing cable force optimization, since the arch rib alignment, tower deviation, cable force uniformity, and safety during construction for long-span arch bridges' cable-stayed buckles are considered. This approach effectively addresses the defects of traditional monitoring and calculation methods. At the same time, this paper writes relevant programs through MATLAB R2016a, which has a fast iteration speed and high calculation efficiency. In addition, the parameters of the hoisting construction were controlled within the permissible range.

For the nonlinear temperature field of an arch rib and buckle system under the combined action of ambient temperature and solar radiation, due to the tangential assembly of the arch rib, the alignment of the arch rib at each segment has a strong connection. The errors of the measured and predicted values predicted by the GM(1, 1) model and the fitting results were within 5% at different temperatures, providing a reference for the alignment control of arch bridges.

Through error feedback control, various parameter errors and environmental interferences in the bridge construction process were corrected and brought within a feasible domain. The accumulated error of each segment during cable-stayed buckles easily leads to the deviation of the arch formation state; this problem has been solved. Moreover, the arch ring's arch formation and bridge formation states both met the requirements. Thus, the construction control problem of long-span arch bridges was solved.

Author Contributions: Conceptualization, X.Y. and M.Y.; methodology, C.L. and L.W.; data curation, X.Z.; writing original draft preparation, T.H. and X.W.; writing-review and editing, X.Y. All authors have read and agreed to the published version of the manuscript.

Funding: This study was partly sponsored by following fund programs: the National Natural Science Foundation of China (code: 51738004); the National Natural Science Foundation of China (code: 51868006); the Scientific and Technological Project of the Science and Technology Department of Guangxi Province (grant number: 2021AC19125).

Data Availability Statement: The original contributions presented in the study are included in the article, further inquiries can be directed to the corresponding author.

Conflicts of Interest: Authors Longlin Wang, Mengsheng Yu, Xiaoli Zhuo and Xirui Wang were employed by the company Guangxi Transportation Science and Technology Group Co., Ltd. Author Tianzhi Hao was employed by the company Guangxi Beitou Traffic Maintenance Technology Group Co., Ltd. The remaining authors declare that the research was conducted in the absence of any commercial or financial relationships that could be construed as a potential conflict of interest.

References

1. Zhao, R.; Zhang, Z. A Summary of Development of Concrete-Filled Steel Tube Framed Arch Bridges in China. *Bridge Constr.* **2016**, *46*, 45–50.
2. Zhou, Q.; Feng, P.; Zhou, J.; Xin, J.; Wang, J. Analysis of concrete emptying in concrete-filled steel tube arch bridge under uneven temperature field. *J. Bridge Constr.* **2024**, *54*, 103–109. [[CrossRef](#)]
3. Mou, T.; Fan, B.; Zhao, Y.; Li, S. Application and Development of Steel Pipe Concrete Bridges in China. *Highway* **2017**, *62*, 161–165.
4. Zhou, Y.; Wang, Y.; Zhou, J. Arch calculation and control method of 500 m class steel pipe arch bridge. *China Highw. J.* **2022**, *35*, 60–72. [[CrossRef](#)]
5. Li, Y.; Li, Y.; Li, J. The calculation method of the whole process cable force optimization of the long-span concrete-filled steel tube arch bridge constructed by cable-stayed suspension method. *Prog. Build. Steel Struct.* **2019**, *21*, 33–39. [[CrossRef](#)]
6. Xie, K.; Wang, H.; Guo, X.; Zhou, J. Study on the safety of the concrete pouring process for the main truss arch structure in a long-span concrete-filled steel tube arch bridge. *Mech. Adv. Mater. Struct.* **2021**, *28*, 731–740. [[CrossRef](#)]

7. Zhen, J.; Wang, J.; Feng, Z.; Han, Y.; Qin, D. Test on vacuum auxiliary filling technology of concrete-filled steel tube arch section. *China Highw. J.* **2014**, *27*, 44–50. [[CrossRef](#)]
8. Han, Y. Test and application of vacuum assisted filling of concrete in tubular arch bridge. *Bridge Constr.* **2015**, *45*, 19–25.
9. Zhou, D.; Deng, N.; Shi, T. Test and numerical simulation analysis of large scale hydration temperature field of concrete-filled steel tube arch bridge. *J. Guangxi Univ.* **2021**, *46*, 51–59. [[CrossRef](#)]
10. Sun, J.; Xie, J. Simulation analysis of the hydration heat of large diameter CFST arch and its effects on loading age. *Appl. Therm. Eng.* **2019**, *150*, 482–491. [[CrossRef](#)]
11. Zhou, Q.; Zhou, J.; Zhang, J.; Zhang, L. Self-regulating loading pouring method of long span CFST arch bridge. *J. Harbin Inst. Technol.* **2020**, *52*, 82–89. [[CrossRef](#)]
12. Zheng, J.; Wang, J. Chinese steel tube concrete arch bridge. *Engineering* **2018**, *4*, 306–331. [[CrossRef](#)]
13. Xu, Y.; Shen, C.; Zhu, Y.; Wang, C. Improved Iteration Algorithm for Determination of Tension of Fastening Stays for Cantilever Construction of Arch Bridge. *Bridge Constr.* **2016**, *46*, 65–69.
14. Qin, D.; Zheng, J.; Du, H.; Han, Y.; Zheng, J.; Wei, L. Optimization Calculation Method for Stayed-Buckle Cable Force under One-Time Tension by Fastening Stay Method and Its Application. *China Railw. Sci.* **2020**, *41*, 52–60.
15. Han, Y.; Qin, D.; Zheng, J. Optimization calculation method for CFST arch bridge cable-stayed suspension construction. *Highway* **2018**, *63*, 100–104.
16. Zhou, J.; Liu, J.; Zhou, W.; Yan, R.; Yan, T. Analysis of the influence of temperature changes on the pre lifting value of cable-stayed buckle and the main arch ring shape of steel tube concrete arch bridges. *J. China Foreign Highw.* **2017**, *37*, 62–66. [[CrossRef](#)]
17. Chen, B.; Wei, J.; Zhou, J.; Liu, J.P. Application of concrete-filled steel tube arch bridges in China: Current status and prospects. *China Civ. Eng. J.* **2017**, *50*, 50. [[CrossRef](#)]
18. Yu, M.; Deng, N.; Wang, L.; Hao, T.; Zhang, Z. Study on Sunshine Temperature Effect in Concrete-filled Steel Tubes Arch Rib of Extra-Large Arch Bridge. *Highw. Eng.* **2021**, *46*, 99–104. [[CrossRef](#)]
19. Liu, X.; Zhou, G.; Qiu, Y. Optimal Polynomial Time-varying Parameters Discrete Grey Model and Its Applications. *Stat. Decis.* **2022**, *38*, 31–36. [[CrossRef](#)]
20. Li, X.; Wang, C. STI prediction based on metabolic GM (1, 1) Copula BP neural network. *Stat. Decis.* **2021**, *37*, 158–161. [[CrossRef](#)]
21. Vasques, J.F.; Goncalves, R.G.D.J.; Silva-Junior, A.J.D.; Martins, R.S.; Gubert, F.; Mendez-Otero, R. Gangliosides in nervous system development, regeneration, and pathologies. *Neural Regen. Res.* **2023**, *18*, 81–86. [[CrossRef](#)]
22. Li, C.; Huang, J.; Li, X. Consider the sunshine temperature field of concrete-filled steel tube arch. *Sino-Foreign Highw.* **2020**, *40*, 102–107.

Disclaimer/Publisher’s Note: The statements, opinions and data contained in all publications are solely those of the individual author(s) and contributor(s) and not of MDPI and/or the editor(s). MDPI and/or the editor(s) disclaim responsibility for any injury to people or property resulting from any ideas, methods, instructions or products referred to in the content.